Published OnlineFirst October 28, 2016; DOI: 10.1158/0008-5472.CAN-16-1797

Molecular and Cellular Pathobiology

Cancer Research

Targeting of PYK2 Synergizes with EGFR Antagonists in Basal-like TNBC and Circumvents HER3-Associated Resistance via the NEDD4–NDRG1 Axis

Nandini Verma[1], Anna-Katharina Müller[1], Charu Kothari[1], Effrosini Panayotopoulou[1], Amir Kedan[1], Michael Selitrennik[1], Gordon B. Mills[2], Lan K. Nguyen[3], Sungyoung Shin[3], Thomas Karn[4], Uwe Holtrich[4], and Sima Lev[1]

Abstract

Triple-negative breast cancer (TNBC) is a highly aggressive, heterogeneous disease with poor prognosis and no effective targeted therapies. EGFR is highly expressed in basal-like TNBC and is considered as a potential therapeutic target. However, EGFR targeting exerts only marginal clinical benefits, possibly due to activation of compensatory signaling pathways, which are frequently associated with HER3 upregulation. Here we show that concomitant targeting of EGFR and the nonreceptor tyrosine kinases PYK2/FAK synergistically inhibits the proliferation of basal-like TNBC cells *in vitro* and attenuates tumor growth in a mouse xenograft model. Dual targeting of EGFR and PYK2/FAK inhibited complementary key growth and survival pathways mediated by AKT, S6K, STAT3, and ERK1/2 activation. PYK2 inhibition also abrogated HER3 upregulation in response to EGFR antagonists, thereby circumventing HER3-associated drug resistance. Mechanistically, PYK2 inhibition facilitated the proteasomal degradation of HER3 while inducing upregulation of NDRG1 (N-myc downstream regulated 1 gene). NDRG1 enhanced the interaction of HER3 with the ubiquitin ligase NEDD4, while PYK2, which interacts with NEDD4 and HER3, interfered with NEDD4–HER3 binding, suggesting that the PYK2–NDRG1–NEDD4 circuit has a critical role in receptor degradation, drug response, and resistance mechanism. Our studies offer a preclinical proof of concept for a strategy of cotargeting the EGFR and PYK2/FAK kinases to improve TNBC therapy. *Cancer Res; 77(1); 86–99. ©2016 AACR.*

Introduction

Triple-negative breast cancer (TNBC) is defined by the absence of both estrogen and progesterone receptors as well as of HER2 amplification (1). EGFR is highly expressed in approximately 50% of patients with TNBC, is implicated in cancer progression and metastasis and considered as a therapeutic target (2). However, single-agent therapy against EGFR did not improve outcome of patients with TNBC (3), possibly due to activation of the compensatory signaling pathway(s). Recent studies suggest that signaling by the c-Met receptor (3), HER3 (4), and AXL (5) can compensate for EGFR inhibition, and that upregulation of HER3 is associated with reduced response to EGFR antagonists in patients with TNBC (6). Upregulation of HER3 was also observed in response to HER2 antagonists in HER2-positive breast cancer and is generally associated with drug resistance to EGFR- and HER2-targeted therapies (7).

Receptor upregulation could be regulated at transcriptional and posttranslational levels (8), including receptor degradation. Knocking down of NEDD4, for example, induced upregulation of HER3 and enhanced breast cancer cell proliferation *in vitro* and tumor growth *in vivo* (9), while AXL degradation can overcome resistance to EGFR antagonists in non–small cell lung cancer (10). Thus, agents that prevent the upregulation of receptor tyrosine kinases (RTK) in response to EGFR antagonists may offer an efficient therapeutic strategy to improve treatment and overcome resistance. Consistent with this concept, previous studies suggest that dual targeting of EGFR and other RTKs that heterodimerize or cross-talk with EGFR signaling could potentiate drug response and/or overcome resistance. Combined targeting of both EGFR and cMet receptors, for example, was proposed as an effective therapeutic strategy for TNBC (3, 11).

Recently, we found that the nonreceptor tyrosine kinase PYK2 is a common downstream effector of EGFR, cMet, and their cross-talk signaling in certain TNBC cell lines (12). PYK2 and its closely related focal adhesion kinase (FAK) are key mediators of various mitogenic and migratory pathways triggered by RTKs, cytokine receptors, and integrin clustering (13).

[1]Department of Molecular Cell Biology, Weizmann Institute of Science, Rehovot, Israel. [2]Department of Systems Biology, The University of Texas MD Anderson Cancer Center, Houston, Texas. [3]Department of Biochemistry and Molecular Biology, Biomedicine Discovery Institute, Monash University, Clayton, Australia. [4]Department of Obstetrics and Gynecology, Goethe University Frankfurt, Frankfurt, Germany.

Note: Supplementary data for this article are available at Cancer Research Online (http://cancerres.aacrjournals.org/).

Corrected online December 20, 2019.

N. Verma, A.-K. Müller, and C. Kothari contributed equally to this article.

Corresponding Author: Sima Lev, Department of Molecular Cell Biology, Weizmann Institute of Science, 234, Herzel st., Rehovot 76100, Israel. Phone: 972-8934-2126; Fax: 972-8934-4125; E-mail: sima.lev@weizmann.ac.il

doi: 10.1158/0008-5472.CAN-16-1797

Published OnlineFirst October 28, 2016; DOI: 10.1158/0008-5472.CAN-16-1797

Both PYK2 and FAK have been implicated in the progression and invasion of diverse human cancers, including breast cancer (14, 15). Small-molecule inhibitors of FAK/PYK2 suppressed tumor growth and metastasis in several preclinical models and have initial clinical activity in patients with limited adverse effects (14).

Recent studies suggest that FAK is frequently highly expressed in TNBC and could be a potential therapeutic target (16), while proteomic analysis suggests that activated PYK2 is mainly found in basal-like breast carcinomas and correlates with high levels of EGFR and activated ERK1/2 (17).

Using clinical specimens, database analysis, functional studies in TNBC cell lines, and murine xenograft models, we show here that high expression of both EGFR and PYK2 in TNBC indicates a poor prognosis. We further show that inhibition of PYK2 and/or FAK substantially sensitized basal-like TNBC to EGFR antagonists, and that dual targeting of EGFR and PYK2/FAK synergistically inhibits cell growth *in vitro* and tumor growth *in vivo*. Furthermore, PYK2 inhibition abolished the upregulation of HER3 in response to EGFR antagonists by facilitating its proteasomal degradation, and bypassed HER3-associated feedback resistance. PYK2 interacts with HER3 and NEDD4 and interferes with HER3–NEDD4 binding. PYK2 knockdown (KD) induces upregulation of NDRG1 (N-myc downstream regulated 1 gene), a protein implicated in tumor suppression and anticancer drug resistance (18), while NDRG1 substantially enhances NEDD4–HER3 binding and consequently HER3 degradation. We propose that the PYK2–NEDD4–NDRG1 circuit plays a central role in HER3 degradation, and that dual targeting of EGFR with PYK2/FAK not only inhibits tumor growth, but also bypasses drug resistance, and thus, could offer a promising, efficient, and beneficial therapeutic strategy for basal-like TNBC.

Materials and Methods

Antibodies, reagents, and chemicals

A complete list of reagents is provided in the Supplementary Information.

Cell culture

MDA-MB-468, MDA-MB-231, BT20, BT549, HCC1937, HCC1143, SUM159PT, Hs578T, and human embryonic kidney (HEK293) cells were obtained from ATCC (2013–2015). HCC-38 was a kind gift from Maire Virginie (Institut Curie, Research Center, Paris, France; 2014). Gefitinib- and erlotinib-resistant cell lines were established as described in the Supplementary Information. The identity of all cell lines was performed by STR profiling every 6 months by the source. Upon receiving, the cells were expanded and subsequently stored in liquid nitrogen. Original vials were thawed for experiments and have only been passaged for up to 2 months. Cell lines were verified to be mycoplasma negative.

shRNA lentivirus production and infection

Two different lentiviruses encoding shRNAs targeting PYK2 were used for PYK2 knockdown as we described previously (19). Two FAK-specific lentiviruses shRNAs were purchased from Sigma and validated for specificity and efficiency (TRCN0000196310 and TRCN0000194984). Other DNA constructs and related procedures are described in Supplementary Information.

Immunoblot analysis

Western blot analysis was performed as described previously (12). A complete list of used antibodies and a detailed procedure is given in the Supplementary Information.

Cell viability and proliferation

Cell proliferation was assessed by MTT (3-(4,5-dimethylthiazolyl-2)-2,5-diphenyltetrazolium bromide) colorimetric assay and by crystal violet (CV) staining as described in the Supplementary Information.

IC_{50} values and drug synergism

Cells in 96-well plates were treated with different drug concentrations as indicated, and dose matrices were applied for drug combination analysis. The cells were treated with drugs for 72 hours and cell viability was measured by MTT. IC_{50} values were determined by the nonlinear regression method using GraphPad Prism version v.5.0 (GraphPad Software). Combination index values (CI) were calculated by CompuSyn software (CompuSyn. Inc) and accordingly, synergistic ($CI < 1$), additive ($CI = 1$), and antagonistic ($CI > 1$) effects were defined.

Breast cancer mouse xenografts

A detailed procedure is given in Supplementary Information. Briefly, 3×10^6 luciferase-expressing control or PYK2-depleted MDA-MB-468 cells were implanted into the mammary gland of female Nu/Nu mice ($n = 50$). Six weeks later when tumors volume reached >75 mm^3, vehicle or gefitinib (100 mg/kg/day) were orally administered. Tumor dimensions were measured by caliper and bioluminescence images acquired weekly. Student *t* test was applied for statistical analysis.

Immunohistochemical staining and analysis

Formalin-fixed paraffin-embedded TNBC sections were processed for IHC as described previously (12). The intensity of the immunohistochemical staining was evaluated semiquantitatively and H-Score was calculated for each sample essentially as we described previously (20). Further experimental details are described in Supplementary Information.

Microarray data

All gene expression data used in the study are publicly available. The accession numbers of the used datasets from GEO and Array Express database are listed in Supplementary Table S1 and direct web links for all used individual samples are given in Supplementary Table S2.

Soft agar colony formation assay

Soft agar colony formation assay was performed as described previously (21). A detailed description of the procedure is given in the Supplementary Information.

Immunofluorescence staining

Immunofluorescence staining was performed as described previously (12). A detailed description of the procedure is given in the Supplementary Information.

Immunoprecipitation

Immunoprecipitation studies were carried out as described previously (22). A detailed procedure is described in the Supplementary Information.

Published OnlineFirst October 28, 2016; DOI: 10.1158/0008-5472.CAN-16-1797

Results

PYK2/FAK depletion attenuates the proliferation of basal-like TNBC cell lines

Previous gene expression and IHC studies showed that FAK is frequently highly expressed in TNBC (16, 23), whereas proteomic analysis demonstrated high levels of phospho-PYK2 and EGFR in basal-like TNBC cell lines (17). These observations led us to characterize the role of PYK2 as well as FAK in TNBC. We screened a panel of 20 commonly studied TNBC cell lines for PYK2, FAK, and EGFR protein expression, and further analyzed the influence of PYK2 and FAK on growth of nine selected cell lines; five have been classified as basal-like (BT-20, MDA-MB-468, HCC1937, HCC38, HCC1143), whereas the other four as mesenchymal or mesenchymal stem-like cell lines (SUM159, Hs578T, MDA-MB-231, BT-549; ref. 24). As shown, all nine TNBC cell lines express moderate-to-high levels of PYK2 and FAK as well as EGFR (Fig. 1A). Depletion of either PYK2 or FAK expression using corresponding lentiviral shRNAs (12, 19) reduced the expression of PYK2 or FAK kinases, and in few cell lines also decreased the steady-state level of EGFR. Depletion of PYK2 or FAK reduced cell growth by 10%–70%. Profound growth-inhibitory effects were obtained in basal-like cell lines compared with mesenchymal lines (Fig. 1B), particularly, in PYK2-depleted BT-20, MDA-MB-468, and HCC1937 cells, which highly express EGFR (Fig. 1A). Importantly, MDA-MB-468 and BT-20 cell lines harbor amplification of *EGFR* gene (25), express high levels of EGFR, and are driven by oncogenic EGFR signaling (26). Together, these results suggest that basal-like TNBC cell lines with high EGFR expression are more susceptible to PYK2 depletion.

PYK2 and/or FAK inhibition synergizes with EGFR antagonists in basal-like TNBC

The profound effect of PYK2 depletion on the proliferation of BT-20, MDA-MB-468, and HCC1937 cell lines (Fig. 1B) suggests that inhibition of PYK2 together with EGFR could have synergistic effects in basal-like TNBC cell lines, and thus, a potential clinical benefit. We therefore examined whether PYK2 or FAK depletion could potentiate the effects of EGFR antagonists. The effect of gefitinib and erlotinib, selective small-molecule EGFR kinase inhibitors (Supplementary Fig. S1A; ref. 27), on cell viability in the five basal-like TNBC cell lines was determined in control and PYK2- or FAK-depleted cells. As shown in Fig. 1C, depletion of PYK2 or FAK substantially reduced (3.5–9 fold) the half maximal inhibitory concentration (IC_{50}) of either gefitinib or erlotinib in MDA-MB-468 and BT-20 cells, compared with other basal-like cell lines (1.1–1.5 fold). Consistent with these results, PYK2 or FAK depletion remarkably reduced viability of gefitinib-treated MDA-MB-468 and BT-20 cells, as demonstrated by crystal violet staining (Fig. 1D). To determine whether PYK2 and/or FAK inhibition synergize with EGFR inhibitors, we used two commercially available FAK inhibitors; PF573228 (PF228), a selective FAK inhibitor (28) and PF431396 (PF396), a dual PYK2/FAK inhibitor (a commercial, selective PYK2 inhibitor is currently not available) (29). These two inhibitors have been previously used in various experimental settings, including preclinical trials (14). We first determined their IC_{50} values in the five basal-like TNBC cell lines (Fig. 1E), and subsequently their synergistic effect with EGFR antagonists (Supplementary Fig. S1B and S1C) using the Chou–Talalay method to calculate their CI (30). As seen in Supplementary Fig. S1B, PF228 synergized with gefitinib in MDA-MB-468 and BT-20 cell lines, as indicated by the CI values (CI < 1). The dual inhibitor PF396 also synergized with gefitinib in MDA-MB-468 and BT-20 and markedly reduced cell growth in gefitinib-treated cells (Fig. 1F). In fact, PF396 potentiated the effect of gefitinib on cell viability and synergized with either gefitinib (Fig. 1G) or erlotinib (Supplementary Fig. S1C) in all the five basal-like TNBC cell lines that were examined. Consistent with these results, concurrent knockdown of both PYK2 and FAK significantly enhanced the effect of gefitinib on HCC1937, HCC1134, and HCC38 cell viability, and profoundly reduced cell growth (Supplementary Fig. S1D). Collectively these results suggest that coinhibition of EGFR with PYK2 and FAK could be an efficient treatment for basal-like TNBC patients with a moderate-to-high expression level of EGFR, while combination of EGFR inhibitors with either PYK2 or FAK inhibition could be sufficient for those with very high EGFR expression, such as MDA-MB-468 and BT-20. Noteworthy, the synergistic effects of gefitinib and the dual PYK2/FAK inhibitor PF396 in MDA-MB-468 and BT-20 cells were stronger compared with previously described drug combinations targeting EGFR and cMet (EMD1214063; ref. 3) in the same cell lines, or EGFR and MEK in MDA-MB-468 (Supplementary Fig. S1E; ref. 31), further emphasizing the potency of EGFR-PYK2/FAK drug combination and its potential clinical implication.

To further demonstrate the potency of the combined targeting of EGFR, PYK2 and/or FAK, we examined the effects of gefitinib (IC_{25}) on the anchorage-independent growth of control, PYK2- or FAK-depleted MDA-MB-468 or BT-20 cells using soft agar assays. As seen in Fig. 1H, although gefitinib, PYK2-, or FAK-KD reduced colony number and size, their combined effects were much more dramatic and almost abolished cell growth in soft agar. Similarly, combination of gefitinib and PF396 remarkably affected the anchorage-independent growth of these cell lines (Supplementary Fig. S1F), consistent with their synergistic effects (Fig. 1G).

PYK2 depletion and EGFR antagonists collaboratively abrogate tumor growth in mouse xenograft model

In light of the profound effect of PYK2 depletion on gefitinib-induced MDA-MB-468 cell death and anchorage-independent growth in soft-agar (Fig. 1C, D, and H), we hypothesized that PYK2 depletion could potentiate the effect of gefitinib on tumor growth *in vivo*. We therefore established an MDA-MB-468 xenograft model using control or PYK2-depleted luciferase-expressing MDA-MB-468 cells. The cells were implanted into the mammary fat pads of athymic nude mice ($n = 25$ of each group). Tumor growth was monitored weekly by whole-body bioluminescence imaging, while gross tumor size was measured by caliper. As shown in Fig. 2A, PYK2 depletion significantly attenuated tumor growth, and 6 weeks after cell implantation, the average tumors volume reached approximately 75 mm^3 in PYK2-depleted cells, whereas approximately 130 mm^3 in the control MDA-MB-468 cells. At this time, the mice were randomly divided into two groups ($n = 12$), of which, one group was treated with gefitinib (100 mg/kg/day) and the second with a vehicle control. The mice were treated for 39 days with gefitinib and tumor growth was monitored weekly. The treatments had no obvious effects on body weight (Fig. 2C), but did affect tumor growth (Fig. 2A and B). As seen in the representative images of mice at the end of the experiment (11.5 weeks; Fig. 2B), PYK2-KD as well as gefitinib treatment reduced tumor size by approximately 30%–40%. Immunohistochemical staining of xenograft tumor sections for proliferating cell nuclear antigen (PCNA; ref. 32) and for cleaved

Published OnlineFirst October 28, 2016; DOI: 10.1158/0008-5472.CAN-16-1797

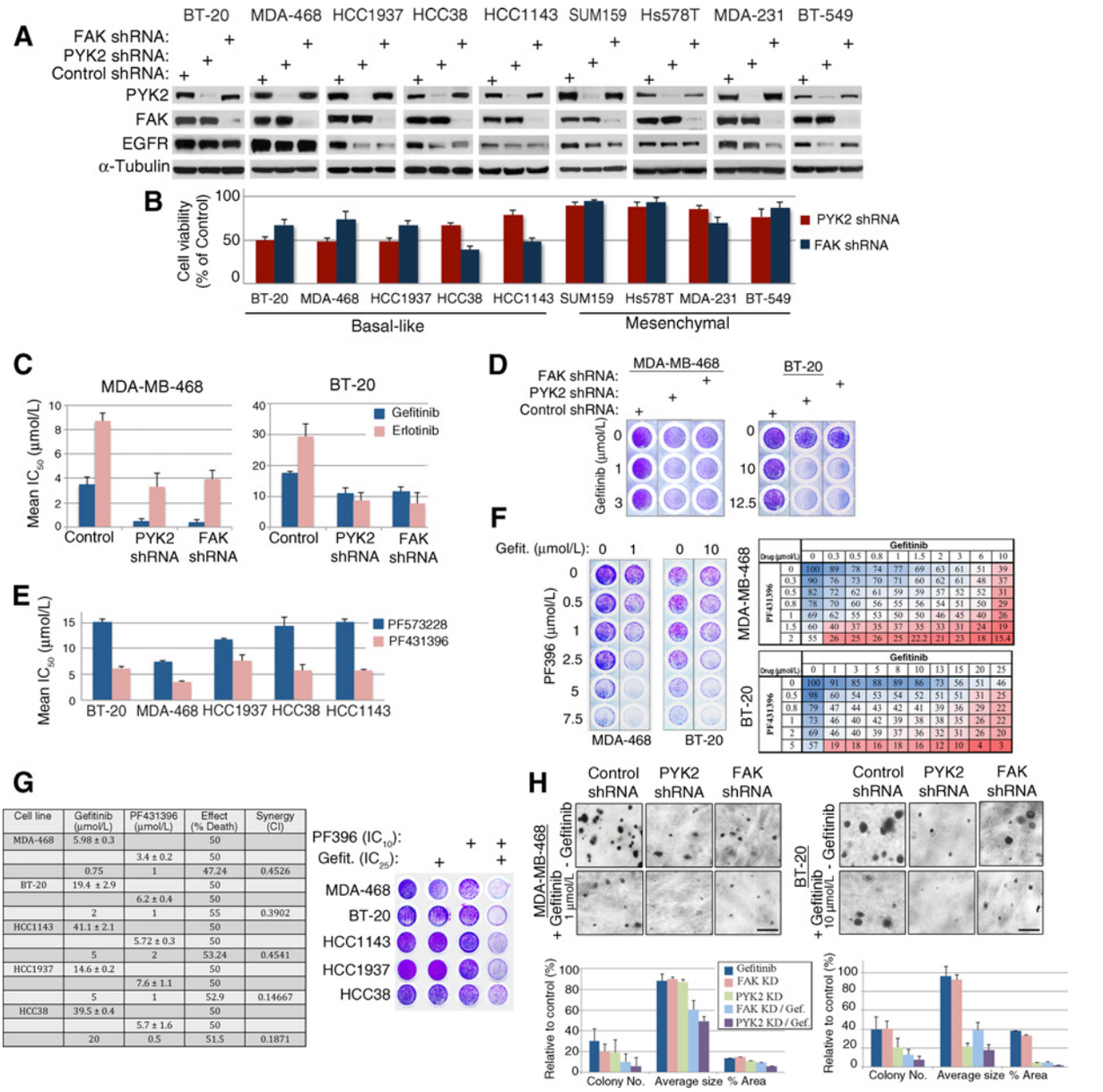

Cell line	Gefitinib (μmol/L)	PF431396 (μmol/L)	Effect (% Death)	Synergy (CI)
MDA-468	5.98 ± 0.3		50	
		3.4 ± 0.2	50	
	0.75	1	47.24	0.4526
BT-20	19.4 ± 2.9		50	
		6.2 ± 0.4	50	
	2	1	55	0.3902
HCC1143	41.1 ± 2.1		50	
		5.72 ± 0.3	50	
	5	2	53.24	0.4541
HCC1937	14.6 ± 0.2		50	
		7.6 ± 1.1	50	
	5	1	52.9	0.14667
HCC38	39.5 ± 0.4		50	
		5.7 ± 1.6	50	
	20	0.5	51.5	0.1871

Figure 1.

Inhibition of PYK2/FAK affects cell proliferation, anchorage-independent growth, and synergizes with EGFR inhibition in basal-like TNBC. **A,** Levels of PYK2, FAK, and EGFR proteins in control and PYK2- or FAK-depleted TNBC cell lines were determined by Western blot analysis using the corresponding antibodies. **B,** Cell viability of control, PYK2-, or FAK-depleted TNBC cell lines was assessed by MTT assay and is presented as percentage of control. Data represents mean values ± SD of three independent experiments. **C** and **D,** PYK2 or FAK-KD potentiates the effect of gefitinib (**C** and **D**) and erlotinib (**C**) on MDA-MB-468 or BT-20 cell death, as determined by IC_{50} values (**C**) and by the colony staining assay (**D**). **E,** The IC_{50} values of the indicated basal-like TNBC cell lines to FAK (PF573228) and FAK/PYK2 (PF431396) small-molecule inhibitors were determined in three independent experiments and mean values ± SD are shown. **F,** Colony formation assay was used to demonstrate the stimulatory effect of PF4313196 on gefitinib-induced MDA-MB-468 or BT-20 cell death. Representative images of crystal violet staining of control and drug-treated cells (72 hours) are shown in the left panels. MTT assay results of dose response matrix of gefitinib and PF431396 drug combinations are shown on the right. Cell viability is presented as percentage of control (untreated cells) and labeled by blue (high)-to-red (low) color code. **G,** IC_{50} values for gefitinib, PF431396, and their combined effects in the indicated basal-like TNBC cell lines. Drug synergy was assessed by the CI values. Right, colony formation assays of the five basal-like TNBC cell lines upon gefitinib and/or PF396 treatment demonstrate the potent combined effects of the drugs. **H,** Anchorage-independent growth of control, PYK2- or FAK-KD MDA-MB-468, and BT-20 cells in the absence or presence of 1 or 10 μmol/L gefitinib, respectively. The colonies were grown for two weeks and then for an additional three weeks in the absence or presence of gefitinib. Quantitative evaluation of total number of colonies, average colony size, and overall area covered with colonies from two independent experiments is shown as percentage of control. Data represent mean ± SD. Representative colonies were photographed using an inverted light microscope. Scale bar, 100 μm.

Published OnlineFirst October 28, 2016; DOI: 10.1158/0008-5472.CAN-16-1797

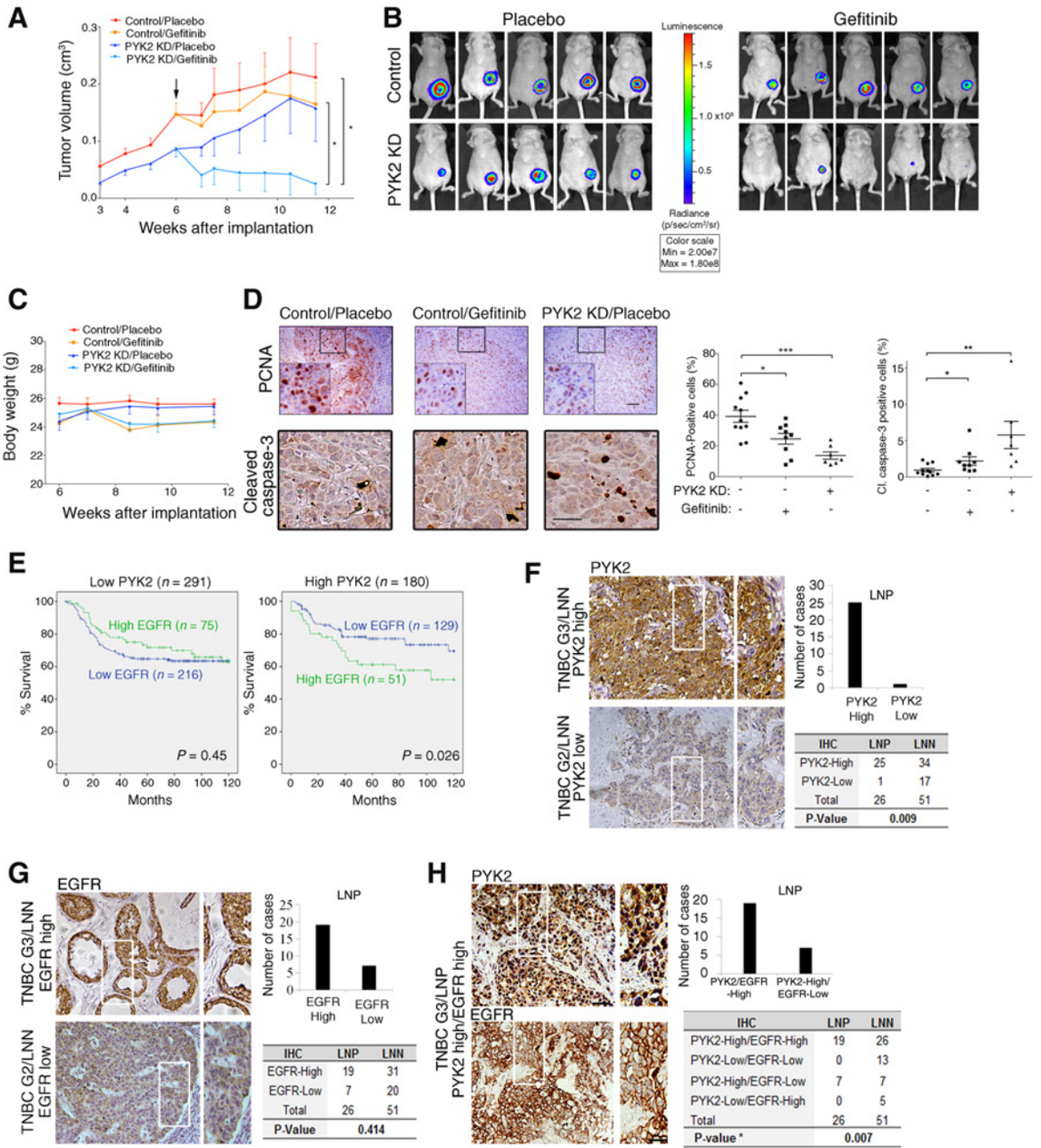

Figure 2.

Combined inhibition of PYK2 and EGFR inhibits tumor growth in mouse xenograft models, whereas high coexpression of PYK2-EGFR in human TNBC samples indicates poor prognosis. **A,** Tumor xenograft growth of control and PYK2-depleted TNBC cells. Control and PYK2-depleted luciferase-expressing MDA-MB-468 cells were implanted into the fourth inguinal mammary glands of 6-week-old nude mice ($n = 50$). Six weeks later (arrow), each group was randomly divided into two; one was treated orally with vehicle (placebo) and the second with gefitinib 100 mg/kg/day for a period of 39 days. Tumor volume (cm^3; **A**) and body weight (g; **C**) were measured at the indicated time points (∼weekly). The value at each time point represents the mean volume of 8–12 tumors; error bars, SEM. Student *t* test, **, $P < 0.01$. **B,** Representative bioluminescent images (IVIS instrument, Living Image 3.0 software) of mice of the four groups described above. Bioluminescent images were acquired once a week throughout the experiment. Pictures shown correspond to the end of the experiment, day 39 post-treatment. **D,** Representative histologic photomicrographs of xenograft tumors (control and PYK2-KD) treated with vehicle or gefitinib and stained with hematoxylin and/or eosin and for PCNA, as a marker for proliferating cells or cleaved caspase-3, as a marker for apoptotic cells. Scale bar, 50 μm. Percentages of PCNA-positive and cleaved caspase-3–positive cells were quantitated by counting approximately 500 cells from 5 highly nucleated, equal microscopic fields for each tumor of the three depicted groups. Data are expressed as mean ± SD. Student *t* test, *, $P < 0.05$; **, $P < 0.01$. **E,** Kaplan–Meier plots of event-free survival of TNBC patients with either low ($n = 291$) or high ($n = 180$) PYK2 expression, which express either high (green) or low (blue) EGFR levels. Strong correlation was obtained between high PYK2/high EGFR expression and reduced event-free survival in TNBC patients ($P = 0.026$). **F** and **G,** PYK2 and EGFR expression levels in TNBC tissue sections were analyzed by IHC. Representative images displaying high and low staining intensity are shown. Scale bar, 50 μmol/L. Number of lymph node positive (LNP) tumors that display high or low staining for PYK2 (**F**) and EGFR (**G**) are shown in the corresponding graphs. **H,** Serial sections of representative high grade-LNP TNBC tissue with high levels of both PYK2 and EGFR. Number of tumors with LNP is shown in the graphs. The correlation between the expression levels (high/low) of PYK2, EGFR or both PYK2 and EGFR, and LNM status is depicted in the tables. Statistical analysis was performed applying χ^2 test.

Published OnlineFirst October 28, 2016; DOI: 10.1158/0008-5472.CAN-16-1797

caspase-3, proliferative, and apoptotic markers, respectively, further demonstrated their inhibitory effects (Fig. 2D). Interestingly, xenograft tumors from PYK2-KD cells had a stronger effect on PCNA and cleaved caspase-3 staining compared with gefitinib-treated or control mice. Most importantly, gefitinib substantially reduced the size of PYK2-depleted MDA-MB-468 tumors, and in most cases, complete tumor remission was observed. These remarkable effects strongly suggest that combined targeting of EGFR and PYK2 could be an efficient therapeutic strategy for a subset of basal-like TNBC patients with high EGFR-expressing tumors.

High expression of both EGFR and PYK2 correlates with poor prognosis in TNBC patients

To evaluate the clinical relevance of PYK2 and EGFR targeting in TNBC, we assessed their expression levels in 1,096 TNBC clinical samples using Affymetrix microarray dataset (Human Genome U133A; ref. 33). Gene expression levels of PYK2 and EGFR were obtained from Affymetrix probeset 203111_s_at (PYK2), and 211607_x_at and 210984_x_at (EGFR; Supplementary Fig. S2A and S2C). A cutoff for "high" PYK2 expression (Supplementary Fig. S2C) as well as "high" and "low" EGFR-expressing tumors (Supplementary Fig. S2B) was defined using the Cutoff Finder application (34). Kaplan–Meier analysis demonstrated that EGFR expression has no prognostic value in this TNBC sample sets (Supplementary Fig. S2D). However, when we first stratified TNBC according to PYK2 expression, we observed a significantly reduced survival of TNBC patients with high EGFR who also expressed high PYK2 levels ($P = 0.026$) but not in those who express low levels of PYK2 ($P = 0.45$; Fig. 2E), suggesting that high expression of both EGFR and PYK2 results in reduced survival and poor prognosis.

To further assess the expression of PYK2 in TNBC and its correlation with EGFR, IHC analysis of 77 TNBC tissue samples was carried out using specific EGFR and PYK2 antibodies. The IHC staining intensity was scored as described in the Materials and Methods section and classified as "high" or "low" expression. Representative images are shown in Fig. 2F–H. Of the total 77 TNBC samples, approximately 77% (59/77) were high-grade and approximately 34% (26/77) were lymph node positive (LNP; Supplementary Fig. S2E). High PYK2 expression was observed in approximately 80% (47/59) of high-grade tumors, and approximately 96% (25/26) of the LNP samples. Significant correlation between lymph node metastasis (LNM) status and high PYK2 expression was determined by χ^2 analysis. As shown, PYK2 expression is strongly correlated ($P = 0.009$) with LNM status (Fig. 2F). In contrast, we could not detect significant correlation between EGFR levels and LNM status ($P = 0.414$) in the 77 TNBC samples (Fig. 2G). However, when we analyzed sections for high expression of both PYK2 and EGFR, we found a very strong correlation ($P = 0.005$) with LNM; all the 19 LNP TNBC samples that exhibit high EGFR also exhibit high PYK2 (100%; Fig. 2H). Collectively, these results suggest that high expression of both PYK2 and EGFR in TNBC is significantly associated with LNM, reduced survival, and has a high prognostic value.

Effects of EGFR antagonist and PYK2/FAK inhibition on HER3 receptor, intracellular signaling, and apoptotic pathways

The potent effect of EGFR antagonists together with PYK2/FAK inhibition (kinase activity/expression) on cell and tumor growth, led us to investigate the underlying mechanism. We first evaluated the influence of PYK2/FAK-KD on predominant survival and proliferative signaling pathways in the five basal-like TNBC cell lines using phospho-specific antibodies against activated AKT, S6-kinase, STAT3, and ERK1/2. The levels of cMet and HER3 receptors, which heterodimerize with EGFR were also assessed. The results showed striking differences between PYK2- and FAK-KD (Fig. 3A). In PYK2-KD cells, the phosphorylation of S6-kinase and its protein level were markedly reduced in all five basal-like TNBC cell lines, while FAK-KD influenced AKT activation in a subset of the lines including MDA-MB-468, HCC38, and HCC1143. PYK2-KD also inhibited STAT3 phosphorylation in all the lines except HCC1143. Remarkably, PYK2-KD substantially reduced the level of HER3 in all the five cell lines, while FAK-KD reduced HER3 levels in only a subset of them (BT-20, HCC1143, and HCC38). However, neither knockdown of PYK2 nor of FAK had a significant effect on ERK1/2 phosphorylation (Fig. 3A). Likewise, the FAK inhibitor (PF228) or the dual PYK2/FAK inhibitor (PF396) had also minor effect on pERK1/2 (Fig. 3A and Supplementary Fig. S3A). In fact, PF396 affects most of the pathways altered by PYK2/FAK-KD (Fig. 3A), including the influence on HER3 and/or cMet levels (Fig. 3B, Supplementary Fig. S3A). In contrast, gefitinib significantly inhibited ERK1/2 phosphorylation in all five basal-like cell lines (Fig. 3B), but apparently had no effect on pERK1/2 in the mesenchymal cell lines (MDA-MB-231, BT-549), consistent with the crucial role of EGFR signaling in basal-like TNBC (35).

The strong effects of PYK2/FAK inhibition (kinase activity/expression) on STAT3, S6K, and in a few cases AKT phosphorylation together with the inhibitory effect of gefitinib on the ERK pathway suggest that combined targeting of EGFR and PYK2/FAK could block key growth and survival pathways and effectively induce cell death. We, therefore, examined the combined effects of the two drugs, gefitinib and PF396 on the above signaling pathways. Because of their synergistic effects (Fig. 1G), they applied together at lower concentrations compared with single drug dose (Fig. 3A and Supplementary Fig. S3A). A representative analysis of the affected pathways in MDA-MB-468 (Fig. 3D) as well as in BT-20–treated cells (Supplementary Fig. S3B) demonstrates the influence of the drugs combination on the AKT, S6K, STAT3 and ERK1/2 pathways, and thus, their complementary influence on multiple critical signaling cascades.

The combined drugs also significantly induced caspase-9 and PARP cleavage. Similarly, PYK2- or FAK-KD enhanced the effect of gefitinib on these apoptotic proteins (Supplementary Fig. S3C). Collectively, these results suggest that combined targeting of EGFR and PYK2/FAK complementarily blocks crucial signaling pathways that regulate growth and survival thereby potentiating apoptotic cell death.

While combined targeting of PYK2/FAK with EGFR can influence multiple downstream signaling pathways (Fig. 3C and Supplementary Fig. S3B), depletion of PYK2 also substantially affects the level of HER3 receptor (Fig. 3A). As upregulation of HER3 is frequently associated with drug resistance (7, 36), we examined the influence of gefitinib treatment (72 hours) on HER3 level in the five basal-like TNBC cell lines using Western blotting (WB) and qRT-PCR. As shown in Fig. 3D, an approximately 2- to 3.5-fold upregulation of HER3 protein was detected in all these lines, with minor effects on its mRNA levels (1–1.5 fold, not shown). Further analysis of predominant signaling pathways in gefitinib-treated MDA-MB-468 cells for 3 or 5 days demonstrated upregulation of HER3 as well as pSTAT3 (~2.5–4.5 fold; Fig. 3E).

Published OnlineFirst October 28, 2016; DOI: 10.1158/0008-5472.CAN-16-1797

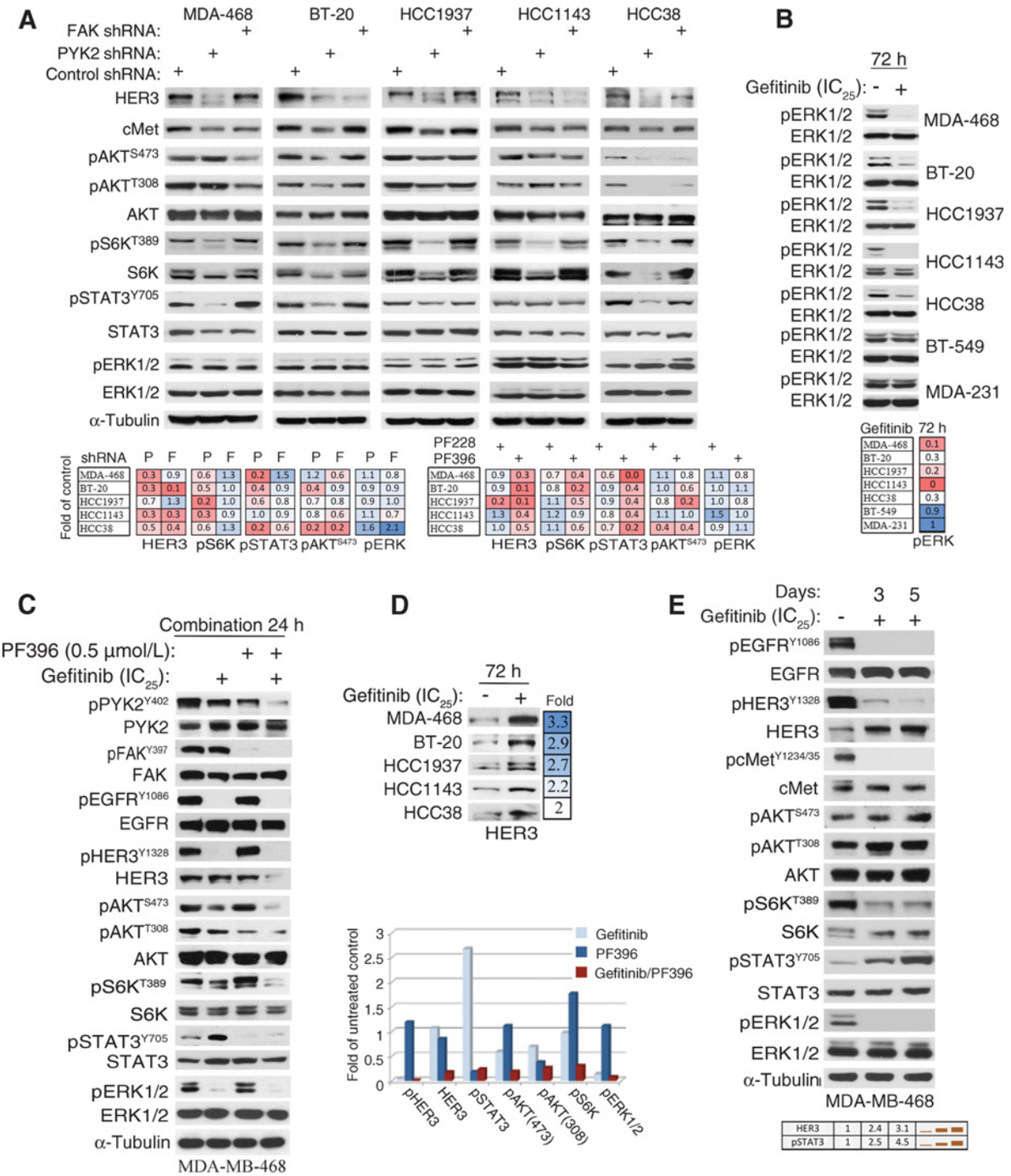

Figure 3.

Effects of PYK2/FAK and EGFR inhibition on multiple survival/proliferative signaling pathways and on HER3 levels. **A,** Effect of PYK- or FAK-KD as well as PYK2/FAK inhibitors (bottom right) on the levels and activation states of the indicated signaling proteins in the five basal-like TNBC cell lines. Shown are representative Western blotting results of reproducible experiments using antibodies against the indicated proteins and their phosphorylated forms. Quantification of protein bands intensities was performed using ImageJ software. Levels of HER3, pS6K, pERK1/2, pSTAT3, and pAKT^{S473} in PYK2- (P) and FAK- (F) knockdown cells or in FAK (PF228) or PYK2/FAK dual (PF396) inhibitor–treated cells as indicated in the bottom right panel were calculated relative to control (fold change) and are shown in the accompanying blue (high)-to-red (low) colored tables. **B,** Gefitinib inhibits ERK1/2 activation in basal-like TNBC. The indicated cell lines were treated with gefitinib (IC_{25}) for 72 hours and ERK activation was assessed by Western blotting using anti-pERK1/2 antibody. Relative pERK1/2 was quantitated as describe above. **C,** Inhibition of PYK2/FAK together with gefitinib affects predominant survival/proliferative signaling pathways. Quantitation of Western blotting results is shown in the bar graph. **D,** Effect of gefitinib on HER3 levels in the five basal-like TNBC cell lines. **E,** Effect of gefitinib treatment for 3 or 5 days on the indicated signaling proteins and pathways. Representative Western blotting results are shown.

Published OnlineFirst October 28, 2016; DOI: 10.1158/0008-5472.CAN-16-1797

Strikingly, both HER3 and pSTAT3 levels are markedly reduced by PYK2-KD or inhibition (Fig. 3A) in these five basal-like TNBC lines. These observations together with the established link between HER3 upregulation and resistance to EGFR antagonists in TNBC patients (6), imply that inhibition of PYK2/FAK not only synergizes with EGFR inhibitors, but could also circumvent HER3-associated resistance in basal-like TNBC.

PYK2 inhibition circumvents HER3-associated resistance to EGFR antagonists

As upregulation of HER3 attenuates antitumor effects of EGFR inhibitors (6), we asked whether its upregulation in basal-like TNBC lines could desensitize the cells to EGFR antagonists, and whether silencing of PYK2/FAK or inhibiting their activity could circumvent these effects. We focused on representative lines, MDA-MB-468 and/or BT-20, and applied three different approaches: short-term treatment with gefitinib for 72 hours (Fig. 4A), long-term treatment with gefitinib (~1.5 months, Fig. 4B), and ectopic HER3 overexpression (Fig. 4C and D). As shown in the corresponding Western blots, HER3 was upregulated by the three different approaches (~2.5–10 fold), and concomitantly pSTAT3 level was increased (Fig. 4A–C). The upregulation of HER3 level was accompanied by reduced sensitivity to gefitinib, and thus, an increase in the IC_{50} (~2–6 fold) in the three different lines (Fig. 4A, B, D tables). Short-term treatment with gefitinib (72 hours, Fig. 4A) markedly increased the IC_{50} (from ~6 μmol/L to ~34 μmol/L) of gefitinib in MDA-MB-468 cells, and combined inhibition of PYK2/FAK using the dual PF396 inhibitor abolished the upregulation of HER3 as well as of pSTAT3, and concomitantly inhibited S6K, AKT, and ERK activation (Fig. 4A). These results suggest that this drug combination effectively blocks predominant survival and proliferative pathways. Likewise, depletion of PYK2 in gefitinib-resistant MDA-MB-468 cells (Fig. 4B) or HER3-overexpressed MDA-MB-468 or BT-20 cells (Fig. 4C) effectively reduced the IC_{50} of gefitinib as well as the activation of S6K, AKT and STAT3 pathways (Fig. 4C). Furthermore, the dual inhibitor PF396 synergized with gefitinib in the three "resistant" cell lines as determined by the calculated CIs (Fig. 4A, B, and D). Together, these results suggest that combined inhibition of EGFR and PYK2/FAK could be an efficient strategy to overcome HER3-associated resistance, possibly due to the profound effect of PYK2 on HER3 levels (Fig. 4A and B).

PYK2 depletion enhances proteasomal degradation of HER3 and concomitantly increases NDRG1 level

The involvement of HER3 in resistance to EGFR antagonists (Fig. 4) together with the profound effect of PYK2-KD as well as the PYK2/FAK dual inhibitor on the steady-state level of HER3 protein in basal-like TNBC cell lines (Fig. 4A and B), led us to investigate the mechanisms by which PYK2 affects HER3 level. We characterized MDA-MB-468 as a representative cell line, as it is highly sensitive to PYK2 depletion/inhibition both *in vitro* and *in vivo* (Figs. 1 and 2A and B). We found that MG132, a proteasome inhibitor, restored the steady-state level of HER3 in PYK2-depleted MDA-MB-468 cells, whereas the lysosomal degradation inhibitor chloroquine had no obvious effect (Fig. 5A), suggesting that PYK2 depletion enhances the proteasomal degradation of HER3. We further examined the subcellular localization of HER3 in control and PYK2-depleted MDA-MB-468 cells. As seen, HER3 was localized to multiple punctuated structures under steady-state conditions, many of which were costained with the recycling endosomal marker Rab11 (Fig. 5B). Interestingly, phospho-PYK2 (pPYK2), which was detected in focal adhesions like structures (12), was also localized to early and recycling endosomes; colocalized with EEA-1 and Rab11, respectively (Fig. 5B). Colocalization between pPYK2 and HER3 was also observed (Fig. 5B). Depletion of PYK2 substantially reduced HER3 immunostaining and the few punctuated HER3-positive structures that observed appeared as Rab11-positive enlarged recycling endosomes (Fig. 5C). Costaining of HER3 and ubiquitin suggests that only a subpopulation of HER3 is ubiquitinated in the control MDA-MB-468 cells. In contrast, HER3 appeared to be highly ubiquitinated in PYK2-KD cells, and MG132 treatment markedly increased the number of HER3-positive structures, further suggesting that PYK2 depletion enhances HER3 ubiquitination and its subsequent degradation (Fig. 5C).

The effect of PYK2 depletion on HER3 degradation together with recent reports describing the effect of NDRG1 on ErbB receptor levels (37), led us to explore a potential link between PYK2 and NDRG1. We first examined the influence of PYK2 or FAK-KD on the steady-state level of NDRG1 as well as its Thr^{346} phosphorylation in the five basal-like TNBC lines. We found that PYK2 depletion strongly induced upregulation of NDRG1 and its phosphorylation in all five lines, while FAK depletion had a slightly less profound effect (Fig. 5D)

Next, we examined whether NDRG1 expression affects the steady-state level of HER3 either by treating MDA-MB-468 cells with di-2-pyridylketone 4,4-dimethyl-3-thiosemicarbazone (Dp44mT; Fig. 5E) or by ectopic expression of NDRG1 and HER3 in HEK293 cells (Fig. 5F). Dp44mT sequesters cellular iron and induces upregulation of NDRG1 (38). As seen in Fig. 5E, Dp44mT substantially increased the levels of NDRG1 and phospho-NDRG1 (pT346) in MDA-MB-468 cells and concomitantly reduced the level of HER3. Likewise, ectopic coexpression of NDRG1 with HER3 in HEK293 cells markedly reduced the level of HER3 (Fig. 5F). Strikingly, however, treatment with MG132 abolished the effect of NDRG1 on HER3, suggesting that similar to PYK2 depletion, NDRG1 expression also enhances the proteasomal degradation of HER3 and enhanced receptor ubiquitination (Fig. 5G).

To further demonstrate the influence of NDRG1 on HER3 level in MDA-MB-468 cells, we knocked down its expression using two different shRNAs. The results shown in Fig. 5H clearly demonstrate the reciprocal effects of NDRG1 and PYK2 on HER3 level. While PYK2-KD increased the level of NDRG1 and decreased the level of HER3, NDRG1-KD increased the level of HER3 and slightly of PYK2 as well.

Collectively, these results establish a novel functional link between HER3 degradation, PYK2, and NDRG1.

The PYK2–NDRG1–NEDD4 axis regulates HER3 degradation

The upregulation of NDRG1 levels in PYK2-depleted cells concomitant with the reciprocal effects of NDRG1 and PYK2 on HER3 levels, suggest that PYK2 affects HER3 levels via NDRG1. To test this, NDRG1 was knocked down in control and PYK2-depleted MDA-MB-468 cells and its influence on HER3 protein level and subcellular distribution was assessed by Western blot analysis (Fig. 6A) and immunofluorescence analysis (Fig. 6B), respectively. As seen in Fig. 6A and B, knockdown of NDRG1 markedly increased the level of HER3 in PYK2-depleted MDA-MB-468 cells. Remarkably, in NDRG1-depleted cells the number and size of HER3-associated punctuated structures were increased and many

Published OnlineFirst October 28, 2016; DOI: 10.1158/0008-5472.CAN-16-1797

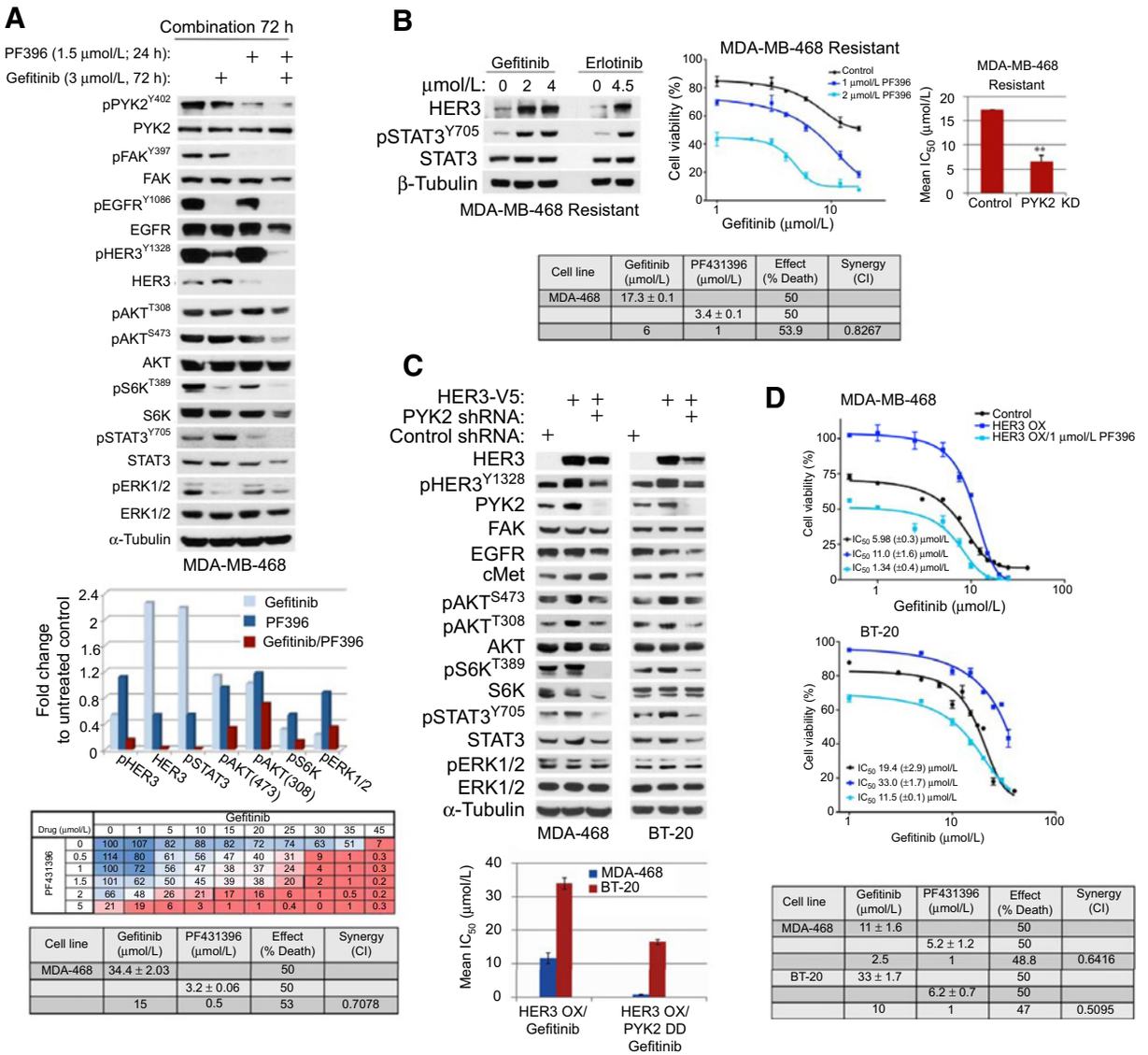

Drug (μmol/L)	Gefitinib 0	1	5	10	15	20	25	30	35	45
PF431396 0	100	107	82	88	82	72	74	63	51	7
0.5	114	80	61	56	47	40	31	9	1	0.3
1	100	72	56	47	38	37	24	4	1	0.3
1.5	101	62	50	45	39	38	20	2	1	0.2
2	66	48	26	21	17	16	6	1	0.5	0.2
5	21	19	6	3	1	1	0.4	0	1	0.3

Cell line	Gefitinib (μmol/L)	PF431396 (μmol/L)	Effect (% Death)	Synergy (CI)
MDA-468	34.4 ± 2.03		50	
		3.2 ± 0.06	50	
	15	0.5	53	0.7078

Cell line	Gefitinib (μmol/L)	PF431396 (μmol/L)	Effect (% Death)	Synergy (CI)
MDA-468	17.3 ± 0.1		50	
		3.4 ± 0.1	50	
	6	1	53.9	0.8267

Cell line	Gefitinib (μmol/L)	PF431396 (μmol/L)	Effect (% Death)	Synergy (CI)
MDA-468	11 ± 1.6		50	
		5.2 ± 1.2	50	
	2.5	1	48.8	0.6416
BT-20	33 ± 1.7		50	
		6.2 ± 0.7	50	
	10	1	47	0.5095

Figure 4.

PYK2/FAK inhibition reduces upregulation of HER3 and its associated resistance to EGFR antagonists. **A,** Short-term gefitinib treatment induces upregulation of HER3 in MDA-MB-468 and desensitizes the cells to gefitinib treatment. Sensitivity to gefitinib was determined by measuring the IC_{50} of gefitinib in gefitinib-pretreated MDA-MB-468 cells. The cells were pretreated with gefitinib (IC_{25}) for 72 hours, gefitinib was washed out, and then cells were incubated for 72 hours with the indicated doses of gefitinib in the absence or presence of PF396 as described in the dose matrix (bottom panel). The IC_{50} values are shown in the table, and synergy was assessed by the CI. Combined effects of gefitinib and PF396 on HER3 levels and downstream signaling pathways were assessed by Western blotting as shown in the top. Quantitation of protein band intensities is shown in the bar graph. **B,** Gefitinib- or erlotinib-resistant cell lines were established as described in Supplementary Information. Levels of HER3, pSTAT3, and STAT3 are shown in the upper Western blot. IC_{50} to gefitinib and synergy with PF396 was determined as described above. The bar graph on the right shows the influence of PYK2-KD on IC_{50} of gefitinib in the gefitinib-resistant MDA-MB-468 cells. **C,** HER3 overexpression desensitizes MDA-MB-468 and BT-20 cells to gefitinib, while knocking down of PYK2 restored sensitivity to gefitinib (graph) and concomitantly reduced HER3 levels in HER3-V5–overexpressed (OX) cells. Western blot analysis shows the effects of HER3-V5-OX and subsequent PYK2-KD on the indicated signaling pathways. The influence of PYK2-KD on the IC_{50} of gefitinib in HER3-OX MDA-MB-468 or BT-20 cells is shown in the accompanying bar graph. **D,** IC_{50} values of gefitinib in HER3-OX MDA-MB-468 and BT-20 cells are shown in the absence and presence of PF396 as indicated. IC_{50} values were calculated and displayed with GraphPad software. Synergism was evaluated by executing CompuSyn software.

of them colocalized with Rab11, while in the double NDRG1/PYK2-KD cells, the number, size, and colocalization of HER3 with Rab11 returned to basal conditions observed in control cells (Figs. 5B and 6B), suggesting that depletion of NDRG1 rescued the effects of PYK2 silencing on HER3 degradation. Reciprocally, we found that PYK2 expression suppressed NDRG1-induced HER3 degradation in its kinase activity–dependent manner (Supplementary Fig. S4A).

Next, we asked how PYK2-NDRG1 regulates HER3 degradation. Previous studies suggest that HER3 ubiquitination and its

Published OnlineFirst October 28, 2016; DOI: 10.1158/0008-5472.CAN-16-1797

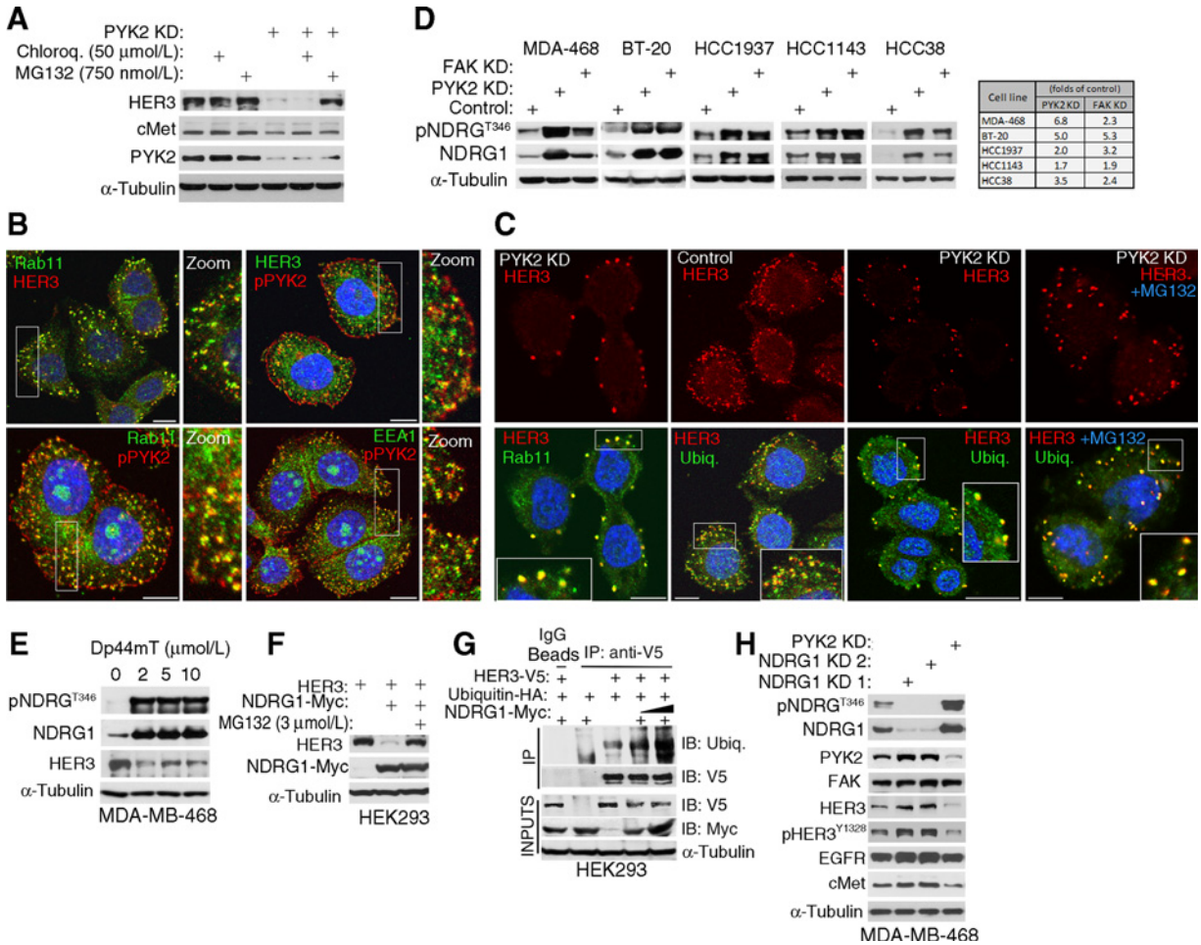

Figure 5.

Depletion of PYK2 accelerates HER3 proteasomal degradation by upregulating NDRG1 expression. **A,** PYK2 depletion results in enhanced HER3 proteasomal degradation. Control and PYK2-depleted MDA-MB-468 cells were treated with chloroquine or MG132 for 12 hours, as indicated. The level of HER3 protein was assessed by Western blotting. **B** and **C,** Subcellular localization of HER3 and pPYK2 was examined by immunofluorescence analysis in control MDA-MB-468 cells (**B**) and/or PYK2-depleted (**C**) cells as indicated. Colocalization with the indicated marker proteins or with ubiquitin (**C**) appears in yellow. Shown are representative confocal images and 2-fold magnified inserts. Scale bar, 10 μm. **D,** Effects of PYK2- or FAK-KD on the protein and phosphorylation (Thr346) levels of NDRG1 in the five basal-like TNBC cell lines. Shown are representative Western blotting results and the levels of NDRG1 in PYK2 and FAK knockdown cells were calculated relative to control (fold change) from three different experiments and are shown in the accompanying table. **E,** The iron chelator Dp44mT induces upregulation of NDRG1 and concurrent downregulation of HER3 protein. MDA-MB-468 cells were treated with the indicated concentrations of Dn44mT for 24 hours. The level of the indicated proteins was assessed by Western blotting. **F,** NDRG1 expression induces proteasomal degradation of HER3. HEK293 cells were transfected with expression vectors encoding HER3 or Myc-tagged NDRG1 and 16 hours later were treated with MG132 (3 μmol/L) for 24 hours, as indicated. The levels of transfected proteins were assessed by Western blot analysis. **G,** NDRG1 enhances the ubiquitination of HER3. HEK293 cells were transfected with the indicated DNA constructs and 16 hours later the cells were treated with MG132 (3 μmol/L) as described above. HER3-V5 was immunoprecipitated (IP) by anti-V5 antibody and its ubiquitination was assessed by Western blotting (IB) using anti-ubiquitin antibody. Input, 10% of total cell lysate used for immunoprecipitation. **H,** Knockdown of NDRG1 results in upregulation of HER3, opposite to PYK2-KD effects. Two different shRNAs were used to knockdown NDRG1. Western blot analysis shows the influence of NDRG1 shRNAs as well as of PYK2-KD on HER3, EGFR and cMet, and on PYK2 and FAK protein levels.

subsequent proteasomal degradation is regulated by two different ubiquitin ligases; Nrdp1, a RING finger E3 ligase (39) and NEDD4, a HECT E3 ligase (9). Further studies have shown a direct link between NDRG1 and NEDD4-2 expression (40). NEDD4-1 and NEDD4-2 are two closely related ubiquitin ligases that regulate the ubiquitination of multiple receptors including ErbB4 (41).

Colocalization studies of HER3 with NEDD4-1 and -2 showed stronger colocalization with NEDD4-2 in MDA-MB-468 cells (Fig. 6C). Interestingly, colocalization between pPYK2 and NEDD4-2 was also observed, suggesting that these two proteins might interact with one another. Most importantly, strong colocalization between HER3 and NEDD4-2 as well as HER3 and NDRG1 was observed in PYK2-depleted MDA-MB-468 cells, and all HER3-positive structures apparently costained with NEDD4-2 or NDRG1 (Fig. 6C). In contrast, depletion of NDRG1 substantially reduced HER3–NEDD4-2 colocalization, suggesting that NDRG1 enhances HER3–NEDD4-2 colocalization and possibly their physical interaction.

To test this, we examined the interactions of HER3 with NEDD4-1/2 by ectopically expressing them in HEK293 cells in

Published OnlineFirst October 28, 2016; DOI: 10.1158/0008-5472.CAN-16-1797

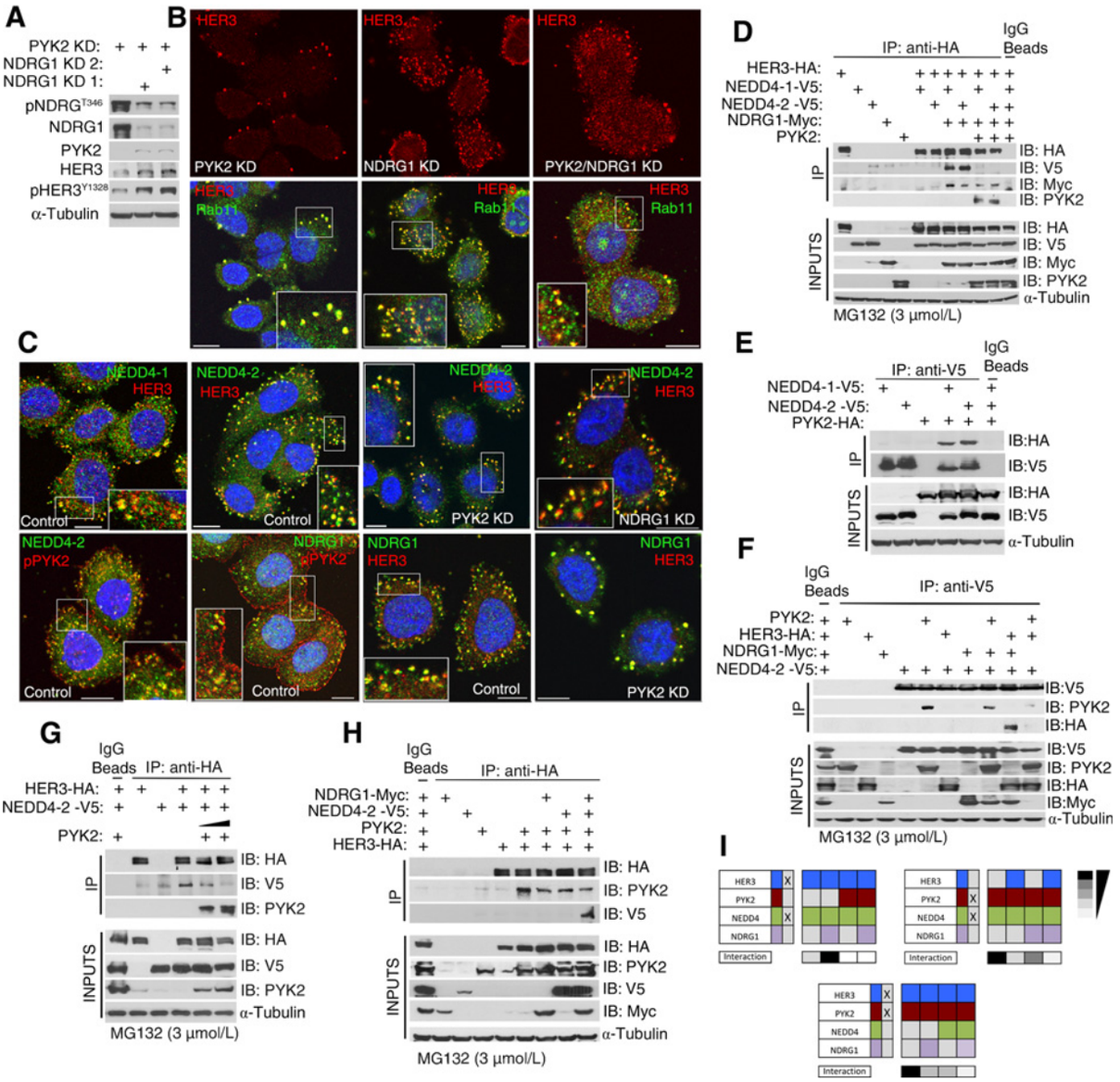

Figure 6.

Interplay between HER3, PYK2, NDRG1, and NEDD4. **A** and **B,** NDRG1 depletion restores HER3 expression in PYK2-KD MDA-MB-468 cells. Shown are representative Western blotting (**A**) and immunofluorescence analysis demonstrating the distribution of HER3 and its colocalization with Rab11 in PYK2 KD, NDRG1 KD, and PYK2/NDRG1 double KD cells (**B**). **C,** The influence of PYK2 or NDRG1 depletion on HER3, NEDD4, and NDRG1 distribution. The left four panels (two rows) demonstrate the distribution and colocalization in control cells. The four right panels demonstrate the effects of PYK2 or NDRG1 depletion on HER3 distribution and its colocalization with NEDD4. Colocalization appears in yellow. Scale bar, 10 μm. Zoomed sections are magnified by two fold. **D,** HER3–NEDD4 interaction is enhanced by NDRG1 and inhibited by PYK2. HEK293 cells were transfected with the indicated DNA constructs. Cells were treated with MG132 as described in Fig. 5. Cells were lysed and HER3 was immunoprecipitated (IP) by anti-HA antibody and its interaction with NEDD4 was determined by Western blot analysis using anti-V5 antibody. Expression levels of the transfected proteins are shown in the input (10% of total lysate). **E,** PYK2 interacts with NEDD4-1/2 as demonstrated by co-IP studies. HEK293 cells were transfected with the indicated DNA constructs. Interactions were assessed by co-IPs as described in **D**. **F,** HER3 and NDRG1 interfere with NEDD4–PYK2 interaction. HEK293 cells were transfected with the indicated DNA constructs. Interactions with NEDD4-V5 were assessed by anti-V5 co-IP studies. **G,** PYK2 and NEDD4 compete for HER3 binding. HEK293 cells were transfected with the indicated DNA constructs. Interactions with HER3-HA were assessed by anti-HA co-IP studies. **H,** NDRG1 and/or NEDD4 affect HER3-PYK2 interaction. HEK293 cells were transfected with the indicated DNA constructs. Interactions with HER3-HA were assessed by anti-HA co-IP studies. **I,** Schematic representation of the protein–protein interactions results shown in panels **D–H**. Strong interactions, black; no/weak interactions, white.

the absence or presence of NDRG1 and/or PYK2. The transfected cells were incubated with MG132 for 24 hours and their interaction was examined by coimmunoprecipitations (co-IP). As shown in Fig. 6D, expression of NDRG1 together with either NEDD4-1/2 markedly enhanced their interaction with HER3. Furthermore, NDRG1 was detected in the same

Published OnlineFirst October 28, 2016; DOI: 10.1158/0008-5472.CAN-16-1797

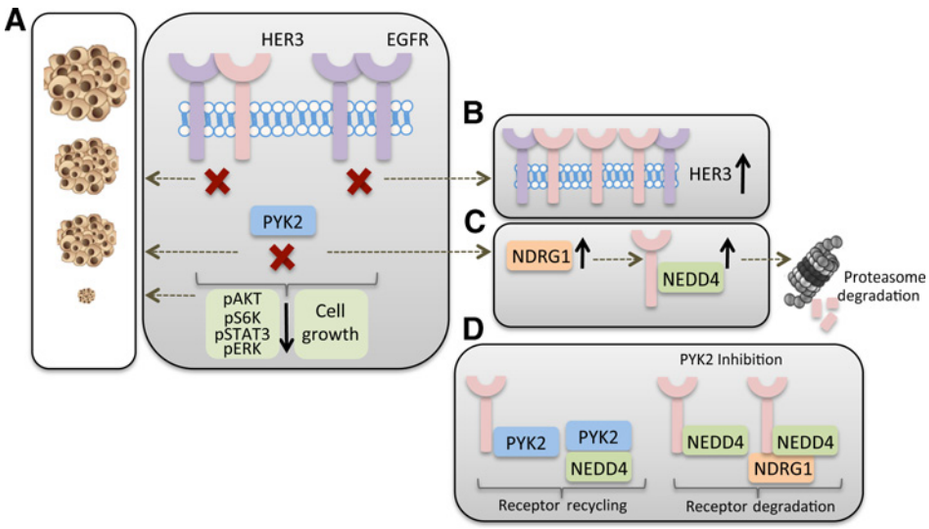

Figure 7.
Inhibition of EGFR and/or PYK2 in basal-like TNBC. **A,** Synergistic effects of the combined EGFR and PYK2 inhibition on cell and tumor growth. **B,** Upregulation of HER3 in response to EGFR antagonists. **C,** PYK2 inhibition induces upregulation of NDRG1, which enhances the ubiquitination of HER3 by NEDD4 and its subsequent proteasomal degradation. **D,** PYK2 binds NEDD4 and HER3 and interferes with NEDD4–HER3 binding, thus PYK2 regulates the degradation of HER3 by enhancing NDRG1 expression and also by competing with NEDD4 binding. In the presence of PYK2, HER3 undergoes recycling, while absence of PYK2 protein or its kinase activity enhances receptor degradation.

immunocomplexes, implying for possible ternary complexes. Expression of PYK2, however, substantially reduced the effect of NDRG1 and apparently abolished the interactions between HER3 and NEDD4-1/2. These results suggest that PYK2 interferes with NEDD4–HER3 binding. On the basis of the localization results (Fig. 6C), we speculated that PYK2 can interact with NEDD4-1/2 and examined this possibility by co-IP experiments. As shown in Fig. 6E, PYK2 and NEDD4-1/2 could be detected in the same immunocomplexes. Similar results were obtained for the endogenous proteins in MDA-MB-468 (not shown). These results suggest that both NEDD4-1/2 (Fig. 6E) and HER3 (Fig. 6D) interact with PYK2. However, the interaction of NEDD4 with PYK2 is slightly reduced in the presence of NDRG1, while NEDD4–HER3 interaction is markedly enhanced by NDRG1 (Fig. 6F). Furthermore, PYK2 inhibits the binding of NEDD4 to HER3 (Fig. 6F), whereas NEDD4 and NDRG1 reduce the binding of PYK2 to HER3 (Fig. 6H), which appears to be dependent on PYK2 kinase activity (Supplementary Fig. S4B). These multiple protein–protein interactions and the complex interplay between PYK2, NDRG1, NEDD4, and HER3, as summarized in Fig. 6I, introduce a new regulatory circuit that affects HER3 fate (Fig. 7). Overall, our findings identified the PYK2–NDRG1–NEDD4 axis as a key regulator of HER3 degradation, and demonstrate its impact on drug response and resistance mechanisms (Fig. 7).

Discussion

TNBC accounts for approximately 20% of all breast cancers and is frequently associated with high mitotic indices, high rates of metastasis, and poor prognosis (42). TNBC is a highly heterogeneous disease comprising distinct molecular subtypes with different clinicopathologic features, metastatic patterns, and therapeutic requirements (1). Six different subtypes possessing unique gene expression patterns and gene ontologies have been identified (24). Basal-like TNBCs (BL1/2) generally expresses specific marker proteins including cytokeratins 5, 6, P-cadherin, p63, and EGFR (43). The high expression of EGFR and its oncogenic role suggest that targeting of EGFR could be an efficient therapeutic approach for basal-like TNBC patients (27). However, targeting of EGFR alone failed to improve survival in clinical trials. Nevertheless, several combination therapies have been recently proposed by both preclinical studies and early-phase clinical trials (ref. 26; https://clinicaltrials.gov/).

In this study, we identified a potent, promising combination therapy for basal-like TNBC, which concomitantly targets EGFR and the PYK2/FAK kinases (Figs. 1 and 2). We show that high expression of both PYK2 and EGFR is significantly associated with poor clinical outcome in TNBC patients (Fig. 2). By using multiple basal-like TNBC cell lines, we show that combined targeting of EGFR and PYK2/FAK synergistically induces cell death *in vitro* (Figs. 1 and 2D and Supplementary Fig. S3C) and remarkably affects tumor growth in animal models (Fig. 2A and B). Analysis of multiple signaling pathways suggest that cotargeting of EGFR and PYK2/FAK complementarily inhibits key growth and survival pathways and consequently induces cell death (Fig. 3C and Supplementary Fig. S3B and S3C). Most strikingly, we found that PYK2-KD as well as PYK2/FAK inhibition affects the steady-state levels of different RTKs, including EGFR (Fig. 1A), cMet, and HER3 (Fig. 3A). The effect on HER3 was obtained in multiple basal-like cell lines (Fig. 3A). This intriguing finding together with the involvement of HER3 in resistance to EGFR antagonists (36) led us to investigate the mechanisms by which PYK2 regulates HER3 levels (Figs. 5 and 6).

Systematic analysis of HER3 levels in control and PYK2-depleted cells revealed that PYK2 depletion enhanced the proteasomal degradation of HER3 (Fig. 5A) and concomitantly induced upregulation of NDRG1 (Fig. 5D). NDRG1 has been identified as a metastasis suppressor in prostate, colon, and breast cancers (44), but its actual physiologic functions remained largely unclear. Nevertheless, previous studies suggest that NDRG1 regulates the endosomal recycling and degradation of different receptors including LDL receptor and E-Cadherin and that it interacts with proteins of the vesicular trafficking machinery (45, 46).

As HER3 constitutively undergoes endocytosis in a clathrin-dependent manner and subsequently recycles to the plasma membrane (47), we hypothesized that PYK2 affects HER3 recycling and inhibits its degradation. Indeed, we found that pPYK2 is localized at both early and recycling endosomes (Fig. 5B), that HER3 is localized to recycling endosomes and that HER3 and pPYK2 colocalize on vesicular-like structures, most likely recycling endosomes (Fig. 5B). In addition, we could detect

colocalization between pPYK2 and NEDD4 and between HER3 and NEDD4 (Fig. 5C), and further demonstrated that both PYK2 and HER3 interact with NEDD4-1/2 (Fig. 6D and E), and also with one another. Finally, we showed that PYK2 interferes with NEDD4–HER3 binding (Fig. 6D and G). These findings not only revealed a new protein–protein interaction network but also suggest that PYK2 inhibits receptor degradation by sequestering its ubiquitin ligase NEDD4 and/or by regulating NDRG1 expression (Figs. 5D and 7). The effect of NDRG1 on NEDD4–HER3 binding (Fig. 6D, F and H) supports this hypothesis, and strongly suggests that the PYK2–NDRG1–NEDD4 axis plays a key role in regulating HER3 fate, thereby affecting drug response and resistance mechanism (Fig. 4).

We propose that this axis not only regulates HER3 trafficking and degradation, but most likely controls the degradation of other cell surface receptors and/or transporters employing similar trafficking/degradation routes. Many membrane proteins have been shown to bind or to be ubiquitinated by NEDD4-1/2 including EGFR, ErbB4, TGFβR1 and various ion channels (48). Our finding that PYK2 interacts with NEDD4-1/2 (Fig. 6E), suggests that PYK2 could regulate the fate of many membrane-associated proteins and thus, could modulate multiple properties of cancer cells, including drug resistance.

Importantly, PYK2 depletion affects EGFR levels in a subset of TNBC lines (Fig. 1A) and also the levels of cMet (Fig. 3A). These two RTKs are also involved in drug resistance and can mediate bidirectional compensatory responses (49). This suggests that inhibition of PYK2 activity/expression not only circumvents HER3-associated drug resistance, but may also overcome EGFR- or cMet-associated drug resistance in specific TNBC subtypes or in response to different targeted therapies.

The potency of PYK2/FAK as therapeutic targets for TNBC, in particular of PYK2, which has not been extensively investigated, is consistent with its high expression in TNBC and its correlation with LNM (Fig. 2F). Furthermore, our results strongly suggest that inhibition of PYK2 activity/expression is prone to overcome drug resistance due to its remarkable effect on the steady state-levels of both RTKs and key intermediate signaling components such as S6K (Fig. 3A). We propose that some of these effects are mediated by NEDD4 and NDRG1. Thus, drugs that efficiently inhibit both PYK2 and FAK are expected to have significant clinical benefit.

In summary, in this study, we not only identified potent combination therapy for basal-like TNBC, but also introduced a new regulatory circuit that plays a crucial role in drug response and resistance mechanisms (Fig. 7). Given that there is no effective treatment for TNBC, and that drug resistance is a major problem of targeted therapies, our studies provide a new and promising therapeutic strategy for this aggressive disease.

Disclosure of Potential Conflicts of Interest

G.B. Mills reports receiving a commercial research grant from Adelson Medical Research Foundation, AstraZeneca, Clinical Outcome Technologies, Komen Research Foundation, Nanostring, Breast Cancer Research Foundation, Karus, Illumina, and Takeda/Millenium Pharmaceuticals, has received speakers bureau honoraria from Symphogen, MedImmune, AstraZeneca, ISIS Pharmaceuticals, Lilly, Novartis, ImmunoMet, Allostery, has ownership interest (including patents), Catena Pharmaceuticals, PTV Ventures, Spindletop Ventures, Myriad Genetics, ImmunoMet, and is a consultant/advisory board member for Adventist Health, AstraZeneca, Provista Diagnostics, Signalchem Lifesciences, Symphogen, Lilly, Novartis, Tarveda, Tau Therapeutics, Allostery, Catena Pharmaceuticals, Critical Outcome Technologies, ISIS Pharmaceuticals, ImmunoMet, Takeda/Millenium Pharmaceuticals, MedImmune, and Precision Medicine. No potential conflicts of interest were disclosed by the other authors.

Authors' Contributions

Conception and design: N. Verma, G.B. Mills, S. Lev

Development of methodology: N. Verma, A.-K. Müller, E. Panayotopoulou

Acquisition of data (provided animals, acquired and managed patients, provided facilities, etc.): N. Verma, A.-K. Müller, C. Kothari, A. Kedan, G.B. Mills, T. Karn, U. Holtrich, S. Lev

Analysis and interpretation of data (e.g., statistical analysis, biostatistics, computational analysis): N. Verma, A.-K. Müller, C. Kothari, E. Panayotopoulou, G.B. Mills, L.K. Nguyen, S. Shin, T. Karn, U. Holtrich

Writing, review, and/or revision of the manuscript: N. Verma, A.-K. Müller, E. Panayotopoulou, A. Kedan, G.B. Mills, L.K. Nguyen, T. Karn, U. Holtrich, S. Lev

Administrative, technical, or material support (i.e., reporting or organizing data, constructing databases): A.-K. Müller

Study supervision: S. Lev

Other (assisted in the animal mice studies, did all the soft agar and colony staining assays as well as all the signaling experiments with pharmacological drug inhibitors, partially performed signaling experiments with PYK2 or FAK-KD, and carried out quantitation of protein band intensities): C. Kothari

Other (helped creating reagents: DNA constructs, viruses and helped with real-time PCR experiments): M. Selitrennik

Other (designed and developed the mathematical model, performed model simulations, and analysis): L.K. Nguyen

Other (designed and developed the mathematical model, performed model simulations, and analysis with L.K. Nguyen): S. Shin

Acknowledgments

Sima Lev is the incumbent of the Joyce and Ben B. Eisenberg Chair of Molecular Biology and Cancer Research. We would like to thank to Moshe Elkabets for productive discussion and excellent suggestions.

Grant Support

This work was supported by the Minerva Foundation, with funding from the Federal German Ministry for Education and Research, and by Dvora and Haim Teitelbaum Endowment Fund. S. Lev is a recipient of grants form Minerva Foundation, Federal German Ministry for Education and Research, and from Dvora and Haim Teitelbaum Endowment Fund.

The costs of publication of this article were defrayed in part by the payment of page charges. This article must therefore be hereby marked *advertisement* in accordance with 18 U.S.C. Section 1734 solely to indicate this fact.

Received June 29, 2016; revised September 22, 2016; accepted October 4, 2016; published OnlineFirst October 28, 2016.

References

1. Peddi PF, Ellis MJ, Ma C. Molecular basis of triple negative breast cancer and implications for therapy. Int J Breast Cancer 2012;2012:217185.
2. Burness ML, Grushko TA, Olopade OI. Epidermal growth factor receptor in triple-negative and basal-like breast cancer: promising clinical target or only a marker? Cancer J 2010;16:23–32.
3. Sohn J, Liu S, Parinyanitikul N, Lee J, Hortobagyi GN, Mills GB, et al. cMET activation and EGFR-directed therapy resistance in triple-negative breast cancer. J Cancer 2014;5:745–53.
4. Sergina NV, Rausch M, Wang D, Blair J, Hann B, Shokat KM, et al. Escape from HER-family tyrosine kinase inhibitor therapy by the kinase-inactive HER3. Nature 2007;445:437–41.

5. Meyer AS, Miller MA, Gertler FB, Lauffenburger DA. The receptor AXL diversifies EGFR signaling and limits the response to EGFR-targeted inhibitors in triple-negative breast cancer cells. Sci Signal 2013;6:ra66.
6. Tao JJ, Castel P, Radosevic-Robin N, Elkabets M, Auricchio N, Aceto N, et al. Antagonism of EGFR and HER3 enhances the response to inhibitors of the PI3K-Akt pathway in triple-negative breast cancer. Sci Signal 2014;7:ra29.
7. Jiang N, Saba NF, Chen ZG. Advances in targeting HER3 as an anticancer therapy. Chemother Res Pract 2012;2012:817304.
8. Garrett JT, Olivares MG, Rinehart C, Granja-Ingram ND, Sanchez V, Chakrabarty A, et al. Transcriptional and posttranslational up-regulation of HER3 (ErbB3) compensates for inhibition of the HER2 tyrosine kinase. Proc Natl Acad Sci U S A 2011;108:5021–6.
9. Huang Z, Choi BK, Mujoo K, Fan X, Fa M, Mukherjee S, et al. The E3 ubiquitin ligase NEDD4 negatively regulates HER3/ErbB3 level and signaling. Oncogene 2015;34:1105–15.
10. Bae SY, Hong JY, Lee HJ, Park HJ, Lee SK. Targeting the degradation of AXL receptor tyrosine kinase to overcome resistance in gefitinib-resistant non-small cell lung cancer. Oncotarget 2015;6:10146–60.
11. Kim YJ, Choi JS, Seo J, Song JY, Lee SE, Kwon MJ, et al. MET is a potential target for use in combination therapy with EGFR inhibition in triple-negative/basal-like breast cancer. Int J Cancer 2014;134:2424–36.
12. Verma N, Keinan O, Selitrennik M, Karn T, Filipits M, Lev S. PYK2 sustains endosomal-derived receptor signalling and enhances epithelial-to-mesenchymal transition. Nat Commun 2015;6:6064.
13. Mitra SK, Hanson DA, Schlaepfer DD. Focal adhesion kinase: in command and control of cell motility. Nat Rev Mol Cell Biol 2005;6:56–68.
14. Sulzmaier FJ, Jean C, Schlaepfer DD. FAK in cancer: mechanistic findings and clinical applications. Nat Rev Cancer 2014;14:598–610.
15. Lipinski CA, Loftus JC. Targeting Pyk2 for therapeutic intervention. Expert Opin Ther Targets 2010;14:95–108.
16. Yom CK, Noh DY, Kim WH, Kim HS. Clinical significance of high focal adhesion kinase gene copy number and overexpression in invasive breast cancer. Breast Cancer Res Treat 2011;128:647–55.
17. Boyd ZS, Wu QJ, O'Brien C, Spoerke J, Savage H, Fielder PJ, et al. Proteomic analysis of breast cancer molecular subtypes and biomarkers of response to targeted kinase inhibitors using reverse-phase protein microarrays. Mol Cancer Ther 2008;7:3695–706.
18. Sun J, Zhang D, Bae DH, Sahni S, Jansson P, Zheng Y, et al. Metastasis suppressor, NDRG1, mediates its activity through signaling pathways and molecular motors. Carcinogenesis 2013;34:1943–54.
19. Selitrennik M, Lev S. PYK2 integrates growth factor and cytokine receptors signaling and potentiates breast cancer invasion via a positive feedback loop. Oncotarget 2015;6:22214–26.
20. Keinan O, Kedan A, Gavert N, Selitrennik M, Kim S, Karn T, et al. The lipid-transfer protein Nir2 enhances epithelial-mesenchymal transition and facilitates breast cancer metastasis. J Cell Sci 2014;127:4740–9.
21. Indo K, Matsuoka T, Nakasho K, Funahashi I, Miyaji H. Reversible induction of anchorage independent growth from normal mouse epidermal keratinocytes, MSK-C3H-NU, in soft agar medium by 12-O-tetradecanoylphorbol-13-acetate and epidermal growth factor. Cancer Res 1988;48:1566–70.
22. Kim S, Leal SS, Ben Halevy D, Gomes CM, Lev S. Structural requirements for VAP-B oligomerization and their implication in amyotrophic lateral sclerosis-associated VAP-B(P56S) neurotoxicity. J Biol Chem 2010;285:13839–49.
23. Glenisson M, Vacher S, Callens C, Susini A, Cizeron-Clairac G, Le Scodan R, et al. Identification of new candidate therapeutic target genes in triple-negative breast cancer. Genes Cancer 2012;3:63–70.
24. Lehmann BD, Bauer JA, Chen X, Sanders ME, Chakravarthy AB, Shyr Y, et al. Identification of human triple-negative breast cancer subtypes and preclinical models for selection of targeted therapies. J Clin Invest 2012;121:2750–67.
25. deFazio A, Chiew YE, Sini RL, Janes PW, Sutherland RL. Expression of c-erbB receptors, heregulin and oestrogen receptor in human breast cell lines. Int J Cancer 2000;87:487–98.
26. Lee MJ, Ye AS, Gardino AK, Heijink AM, Sorger PK, MacBeath G, et al. Sequential application of anticancer drugs enhances cell death by rewiring apoptotic signaling networks. Cell 2012;149:780–94.
27. Corkery B, Crown J, Clynes M, O'Donovan N. Epidermal growth factor receptor as a potential therapeutic target in triple-negative breast cancer. Ann Oncol 2009;20:862–7.
28. Slack-Davis JK, Martin KH, Tilghman RW, Iwanicki M, Ung EJ, Autry C, et al. Cellular characterization of a novel focal adhesion kinase inhibitor. J Biol Chem 2007;282:14845–52.
29. Han S, Mistry A, Chang JS, Cunningham D, Griffor M, Bonnette PC, et al. Structural characterization of proline-rich tyrosine kinase 2 (PYK2) reveals a unique (DFG-out) conformation and enables inhibitor design. J Biol Chem 2009;284:13193–201.
30. Chou TC. Drug combination studies and their synergy quantification using the Chou-Talalay method. Cancer Res 2010;70:440–6.
31. Maiello MR, D'Alessio A, Bevilacqua S, Gallo M, Normanno N, De Luca A. EGFR and MEK blockade in triple negative breast cancer cells. J Cell Biochem 2015;116:2778–85.
32. Kubben FJ, Peeters-Haesevoets A, Engels LG, Baeten CG, Schutte B, Arends JW, et al. Proliferating cell nuclear antigen (PCNA): a new marker to study human colonic cell proliferation. Gut 1994;35:530–5.
33. Hanker LC, Rody A, Holtrich U, Pusztai L, Ruckhaeberle E, Liedtke C, et al. Prognostic evaluation of the B cell/IL-8 metagene in different intrinsic breast cancer subtypes. Breast Cancer Res Treat 2013;137:407–16.
34. Budczies J, Klauschen F, Sinn BV, Gyorffy B, Schmitt WD, Darb-Esfahani S, et al. Cutoff Finder: a comprehensive and straightforward Web application enabling rapid biomarker cutoff optimization. PLoS One 2012;7:e51862.
35. Ueno NT, Zhang D. Targeting EGFR in triple negative breast cancer. J Cancer 2011;2:324–8.
36. Ma J, Lyu H, Huang J, Liu B. Targeting of erbB3 receptor to overcome resistance in cancer treatment. Mol Cancer 2014;13:105.
37. Kovacevic Z, Menezes SV, Sahni S, Kalinowski DS, Bae DH, Lane DJ, et al. The metastasis suppressor, N-MYC downstream-regulated gene-1 (NDRG1), down-regulates the ErbB family of receptors to inhibit downstream oncogenic signaling pathways. J Biol Chem 2016;291:1029–52.
38. Le NT, Richardson DR. Iron chelators with high antiproliferative activity up-regulate the expression of a growth inhibitory and metastasis suppressor gene: a link between iron metabolism and proliferation. Blood 2004;104:2967–75.
39. Qiu XB, Goldberg AL. Nrdp1/FLRF is a ubiquitin ligase promoting ubiquitination and degradation of the epidermal growth factor receptor family member, ErbB3. Proc Natl Acad Sci U S A 2002;99:14843–8.
40. Kovacevic Z, Chikhani S, Lui GY, Sivagurunathan S, Richardson DR. The iron-regulated metastasis suppressor NDRG1 targets NEDD4L, PTEN, and SMAD4 and inhibits the PI3K and Ras signaling pathways. Antioxid Redox Signal 2013;18:874–87.
41. Carraway KLIII. E3 ubiquitin ligases in ErbB receptor quantity control. Semin Cell Dev Biol 2010;21:936–43.
42. Foulkes WD, Smith IE, Reis-Filho JS. Triple-negative breast cancer. N Engl J Med 2012;363:1938–48.
43. Paredes J, Lopes N, Milanezi F, Schmitt FC. P-cadherin and cytokeratin 5: useful adjunct markers to distinguish basal-like ductal carcinomas in situ. Virchows Arch 2007;450:73–80.
44. Kovacevic Z, Richardson DR. The metastasis suppressor, Ndrg-1: a new ally in the fight against cancer. Carcinogenesis 2006;27:2355–66.
45. Pietiainen V, Vassilev B, Blom T, Wang W, Nelson J, Bittman R, et al. NDRG1 functions in LDL receptor trafficking by regulating endosomal recycling and degradation. J Cell Sci 2013;126:3961–71.
46. Kachhap SK, Faith D, Qian DZ, Shabbeer S, Galloway NL, Pili R, et al. The N-Myc down regulated Gene1 (NDRG1) Is a Rab4a effector involved in vesicular recycling of E-cadherin. PLoS One 2007;2:e844.
47. Sak MM, Breen K, Ronning SB, Pedersen NM, Bertelsen V, Stang E, et al. The oncoprotein ErbB3 is endocytosed in the absence of added ligand in a clathrin-dependent manner. Carcinogenesis 2012;33:1031–9.
48. Goh LK, Sorkin A. Endocytosis of receptor tyrosine kinases. Cold Spring Harb Perspect Biol 2013;5:a017459.
49. Logue JS, Morrison DK. Complexity in the signaling network: insights from the use of targeted inhibitors in cancer therapy. Genes Dev 2012;26:641–50.

Correction: Targeting of PYK2 Synergizes with EGFR Antagonists in Basal-like TNBC and Circumvents HER3-Associated Resistance via the NEDD4–NDRG1 Axis

Nandini Verma, Anna-Katharina Müller, Charu Kothari, Effrosini Panayotopoulou, Amir Kedan, Michael Selitrennik, Gordon B. Mills, Lan K. Nguyen, Sungyoung Shin, Thomas Karn, Uwe Holtrich, and Sima Lev

In the original version of this article (1), two instances of inadvertent duplication of crystal violet staining images occurred in Fig. 1D (control shRNA conditions in MDA-MB-468 and BT-20) and in Fig. 1F (0 μmol/L gefitinib control conditions in MDA-468 and BT-20). In addition, the same set of STAT3 Western blot bands was inadvertently duplicated in Fig. 3A (BT-20 and HCC1937). These errors have been corrected in the latest online HTML and PDF versions of the article. The authors regret these errors.

Reference

1. Verma N, Müller AK, Kothari C, Panayotopoulou E, Kedan A, Selitrennik M, et al. Targeting of PYK2 synergizes with EGFR antagonists in basal-like TNBC and circumvents HER3-associated resistance via the NEDD4–NDRG1 axis. Cancer Res 2017;77:86–99.

Published online January 15, 2020.
Cancer Res 2020;80:362
doi: 10.1158/0008-5472.CAN-19-3573

Published OnlineFirst October 28, 2016; DOI: 10.1158/0008-5472.CAN-16-1797

Cancer Research
The Journal of Cancer Research (1916–1930) | The American Journal of Cancer (1931–1940)

AACR American Association for Cancer Research

Targeting of PYK2 Synergizes with EGFR Antagonists in Basal-like TNBC and Circumvents HER3-Associated Resistance via the NEDD4–NDRG1 Axis

Nandini Verma, Anna-Katharina Müller, Charu Kothari, et al.

Cancer Res 2017;77:86-99. Published OnlineFirst October 28, 2016.